Reverse Engineering of an Affinity-Switchable Molecular Interaction Characterized by Atomic Force Microscopy Single-Molecule Force Spectroscopy†

Dario Anselmetti,*,‡ Frank Wilco Bartels,‡ Anke Becker,§ Björn Decker,|| Rainer Eckel,‡ Matthew McIntosh,§ Jochen Mattay,|| Patrik Plattner,⊥ Robert Ros,‡ Christian Schäfer,|| and Norbert Sewald⊥

Experimental Biophysics & Applied Nanoscience, Department of Physics; Transcriptomics, CeBiTec; Organic Chemistry, and Bioorganic Chemistry, Department of Chemistry, Bielefeld University, D-33615 Bielefeld, Germany

Received August 3, 2007. In Final Form: October 17, 2007

Tunable and switchable interaction between molecules is a key for regulation and control of cellular processes. The translation of the underlying physicochemical principles to synthetic and switchable functional entities and molecules that can mimic the corresponding molecular functions is called reverse molecular engineering. We quantitatively investigated autoinducer-regulated DNA−protein interaction in bacterial gene regulation processes with single atomic force microscopy (AFM) molecule force spectroscopy in vitro, and developed an artificial bistable molecular host−guest system that can be controlled and regulated by external signals (UV light exposure and thermal energy). The intermolecular binding functionality (affinity) and its reproducible and reversible switching has been proven by AFM force spectroscopy at the single-molecule level. This affinity-tunable optomechanical switch will allow novel applications with respect to molecular manipulation, nanoscale rewritable molecular memories, and/or artificial ion channels, which will serve for the controlled transport and release of ions and neutral compounds in the future.

Introduction

Regulation and control on a molecular level is a key issue in understanding complex and hierarchic phenomena in cellular processes as well as for future applications of synthetic molecules with tailored architectures and functionalities.[1] Modulating and switching of a molecular interaction is always accompanied by a change in structural conformation and chemical activity. Switching concepts include the reversible transition between two structural molecular isomers by external signals such as electromagnetic fields, mechanical stimuli, or chemical potentials, or the structural modification of the molecule by kinase-driven phosphorylation or effector-induced transformations. In reverse molecular engineering, the underlying physicochemical principles of biological regulation and switching are translated to synthetic and switchable functional entities that can mimic the corresponding molecular function.

During the past two decades, atomic force microscopy (AFM)[2] and AFM-based dynamic force spectroscopy (DFS)[3] have developed into highly sensitive tools for structural and functional investigation of the interaction between and within single biomolecules. Molecular interaction experiments between ligand−receptor,[4] complementary DNA strands,[5] antibody−antigens,[6−8] cell adhesion molecules,[9−11] protein−DNA,[12−15] and supramolecular host−guest complexes[16−19] impressively proved that, beside molecular interaction forces, molecular elasticities, and binding energy landscapes, kinetic reaction off-rate constants could be reproducibly measured in an affinity range from $K_d = 10^{-5}-10^{-15}$ M (K_d: dissociation constant) in various liquid and physiological environments at a sensitivity level of single point mutations. Moreover, mechanosensitive single-molecule transition phenomena have been investigated with AFM force spectroscopy that are based on the conformational switching of (bio)polymeric molecules by UV light[20] and chemical redox reactions.[21,22]

† Part of the Molecular and Surface Forces special issue.

* To whom correspondence should be addressed. E-mail: dario.anselmetti@physik.uni-bielefeld.de.

‡ Experimental Biophysics & Applied Nanoscience.

§ Transcriptomics.

|| Organic Chemistry.

⊥ Bioorganic Chemistry.

(1) Krauss, G. *Biochemistry of Signal Transduction and Regulation*; Wiley-VCH: Weinheim, Germany, 2003.

(2) Hörber, J. K. H.; Miles, M. J. *Science* **2003**, *302*, 1002−1005.

(3) Bustamante, C.; Macosko, J. C.; Wuite, G. J. *Nat. Rev. Mol. Cell Biol.* **2000**, *1*, 130−136.

(4) Florin, E.-L.; Moy, V. T.; Gaub, H. E. *Science* **1994**, *264*, 415−417.

(5) Lee, G. U.; Chrisey, L. A.; Colton, R. J. *Science* **1994**, *266*, 771−773.

(6) Dammer, U.; Hegner, M.; Anselmetti, D.; Wagner, P.; Dreier, M.; Huber, W.; Güntherodt, H.-J. *Biophys. J.* **1996**, *70*, 2437−2441.

(7) Hinterdorfer, P.; Baumgartner, W.; Gruber, H.; Schilcher, K.; Schindler, H. *Proc. Natl. Acad. Sci. U.S.A.* **1996**, *93*, 3477−3481.

(8) Ros, R.; Schwesinger, F.; Anselmetti, D.; Kubon, M.; Schäfer, R.; Plückthun, A.; Tiefenauer, L. *Proc. Natl. Acad. Sci. U.S.A.* **1998**, *95*, 7402−7405.

(9) Dammer, U.; Popescu, O.; Wagner, P.; Anselmetti, D.; Güntherodt, H.-J.; Misevic, G. N. *Science* **1995**, *267*, 1173−1175.

(10) Fritz, J.; Katopodis, A. G.; Kolbinger, F.; Anselmetti, D. *Proc. Natl. Acad. Sci. U.S.A.* **1998**, *95*, 12283−12288.

(11) Zhang, X.; Craig, S. E.; Kirby, H.; Humphries, M. J.; Moy, V. T. *Biophys. J.* **2004**, *87*, 3470−3478.

(12) Bartels, F. W.; Baumgarth, B.; Anselmetti, D.; Ros, R.; Becker, A. *J. Struct. Biol.* **2003**, *143*, 145−152.

(13) Kühner, F., Costa, L. T.; Bisch, P. M.; Thalhammer, S.; Heckl, W. M.; Gaub, H. E. *Biophys. J.* **2004**, *87*, 2683−2690.

(14) Baumgarth, B.; Bartels, F. W.; Anselmetti, D.; Becker, A.; Ros, R. *Microbiol.* **2005**, *151*, 259−268.

(15) Bartels, F. W.; McIntosh, M.; Fuhrmann, A.; Metzendorf, Ch.; Plattner, P.; Sewald, N.; Anselmetti, D.; Ros, R.; Becker, A. *Biophys. J.* **2007**, *92*, 4391−4400.

(16) Schönherr, H.; Beulen, M. W. J.; Bügler, J.; Huskens, J.; van Veggel, F. C. J. M.; Reinhoudt, D. N.; Vancso, G. J. *J. Am. Chem. Soc.* **2000**, *122*, 4963−4967.

(17) Auletta, T.; de Jong, M. R.; Mulder, A. F.; van Veggel, C. J. M.; Huskens, J.; Reinhoudt, D. N., Zou, S.; Zapotoczny, S.; Schönherr, H.; Vancso, G. J.; Kuipers, L. *J. Am. Chem. Soc.* **2004**, *126*, 1577−1584.

(18) Eckel, R.; Ros, R.; Decker, B.; Mattay, J.; Anselmetti, D. *Angew. Chem., Int. Ed.* **2005**, *44*, 484−488.

(19) Schäfer, C.; Eckel, R.; Ros, R.; Mattay, J.; Anselmetti, D. *J. Am. Chem. Soc.* **2007**, *129*, 1488−1489.

(20) Hugel, T.; Holland, N. B.; Cattani, A.; Moroder, L.; Seitz, M.; Gaub, H. E. *Science* **2002**, *296*, 1103−1106.

10.1021/la702373b CCC: $40.75
Published on Web 12/07/2007

In this article, we report how AFM single-molecule force spectroscopy experiments were used in vitro to quantitatively investigate autoinducer-regulated DNA−protein interaction in the gene regulation processes of *Sinorhizobium meliloti*, an α-proteobacterium that fixates atmospheric dinitrogen to ammonia in a symbiotic association with certain genera of leguminous plants.[15] Furthermore, we synthesized and investigated an artificial bistable resorcin[4]arene host−guest system that can be controlled and switched by an external signal (UV light exposure).[18−19] The intermolecular binding functionality (affinity) and its reproducible and reversible switching has again been proven by AFM force spectroscopy at the single-molecule level.[19] Here, we review our recently published original work[15,18,19] from a viewpoint of molecular reverse engineering, where the supramolecular affinity-tunable optomechanical switch allows the control of a specific interaction, and functionally mimics the reported biological protein−DNA interaction.

Materials and Methods

AFM Force Spectroscopy and Data Analysis. Single-molecule force spectroscopy measurements were performed with a custom-made AFM force spectroscopy setup that is based on a commercial AFM (Multimode IIIa, Veeco Instruments, Santa Barbara, CA) at 25 °C in a dedicated liquid cell (binding buffer for DNA−protein, and ethanol for host−guest system). The AFM cantilever deflection force signal and the vertical movement of the piezoelectric transducing element was controlled by a 16 bit AD/DA card (PCI-6052E, National Instruments, Austin, TX) and a high-voltage amplifier (600H, NanoTechTools, Echandens, Switzerland) via an in-house software based on Labview (National Instruments). The deflection signal was low-pass filtered (<6 kHz) by default and box-averaged by a factor of 5−10, giving a typical experimental data set of 2500 points per force−distance curve.

Si_3N_4 cantilevers (MSCT-AUHW, Veeco Instruments or OMCL-TR400PSA-HW, Olympus, Tokyo, Japan) with spring constants ranging from 8 to 16 pN/nm (Veeco) and 18 to 26 pN/nm (Olympus) were used. The spring constants of all AFM cantilevers were calibrated by the thermal fluctuation method[23] with an absolute uncertainty of approximately 15%.

In loading rate-dependent force spectroscopy experiments, the retract velocity of the piezo was varied while the approach velocity was kept constant. Measured force−distance curves were quantitatively analyzed with an in-house Mathlab program (MathWorks, Natick, MA) and corrected to display the actual molecular distances calculated from the *z* piezo position. In order to calculate the loading rate, the respective retract velocity was multiplied by the molecular elasticity, which was determined from the slope of the (corrected) force−distance curves on the last 20 data points before the dissociation events.

The force histograms typically included 100−200 dissociation events that were recorded and analyzed at 5−9 different retract velocities ranging typically from 100 to 6000 nm/s (the approach velocity was typically kept constant at 3000 nm/s). The respective dissociation forces were determined as the maximum of the corresponding force histogram.

The measured data is analyzed in accordance with the standard model for force spectroscopy theory,[24−25] where the mechanically driven dissociation process obeys the law of a thermally activated decay of a metastable state with the following fitting function:

$$F = \frac{k_B T}{x_\beta} \ln \frac{x_\beta r}{k_B T k_{off}}$$

wherein F, $k_BT = 4.114$ pN nm (at 298 K), r, and k_{off} denote the measured dissociation force, thermal energy with Boltzmann factor, loading rate, and thermal off-rate under zero load, respectively. The reaction length x_β defines the distance between the potential well minimum and the metastable energy barrier maximum of the transition state along the reaction coordinate.

Sample Surface and AFM Tip Chemistry. For AFM force spectroscopy experiments, sample surfaces and AFM tips were functionalized as described previously.[15] Briefly, Si_3N_4 cantilevers were first activated by being dipped for 10 s in concentrated nitric acid and silanized in a solution of 2% aminopropyltriethoxysilane (Sigma-Aldrich) in dry toluene for 2 h. After being washed with toluene, the cantilevers were incubated with 1 mM *N*-hydroxysuccinimide−poly(ethylene glycol)−maleimide (PEG) (Nektar, Huntsville, AL) in 0.1 M potassium phosphate buffer, pH 8.0, for 30 min at room temperature.

(a) For the protein−DNA experiments,[15] the cantilevers were washed with phosphate buffer and incubated with 10 ng/μL of the DNA target sequence (see above) bearing a sulfhydryl label in binding buffer solution (100 mM K_2HPO_4/KH_2PO_4, pH 7.5) overnight at 4 °C. The cantilevers were washed with binding buffer and used for force spectroscopy experiments. Modified tips were usable for at least one week if stored at 4 °C. Mica surfaces (Provac AG, Balzers, Liechtenstein) were silanized with aminopropyltriethoxysilane in an exsiccator and incubated with 4 μM $(His)_6$ExpR protein and 20 μM bis(sulfosuccinimidyl)suberate-sodium salt (Sigma-Aldrich) in 0.1 M potassium phosphate buffer, pH 7.5, for 1 h at 4 °C. The sample was washed with binding buffer afterward. Modified surfaces were stable for at least 2 days if stored at 4 °C.

(b) For the supramolecular host−guest experiments,[18−19] the cantilevers were washed with water and functionalized by being incubated overnight at room temperature with a 1 mM ethanol solution of 2-mercaptoethylamine hydrochloride (Sigma-Aldrich). Modified tips were stored at 4 °C and remained usable for at least one week. Prior to use in experiment, the cantilevers were washed with ethanol. Gold-coated sample substrates (11 × 11 mm^2, Arrandee, Werther, Germany) were incubated with the supramolecular calixarene compound and dodecyl sulfide in a molar ratio of 1:40, solubilized in ethanol/chloroform (1:1), by heating to 60 °C for at least 16 h, which is essential for obtaining highly ordered monolayers.

Photoisomerization. Switching of the supramolecular host−guest system from closed to open isomer was performed by heating the sample to 60 °C for 2 h. Closing of the cavity was achieved by irradiation with a quartz halogen UV light source (Norland Opticure 4) for 5 min, yielding 50 mW cm^{-2} in the UV spectral range from 340 to 400 nm. An optical filter ((368.3 ± 7.1) nm, UV-PIL, Schott) was prefixed to the UV source.

Biochemicals. (a) The expression, purification, and characterization of ExpR protein, the organic synthesis of the *N*-acyl homoserine lactone (AHL) autoinducers, and the corresponding specific DNA target sequence were described in details elsewhere.[15] Briefly, ExpR with an N-terminal His tag ($(His)_6$-ExpR) was overexpressed in *Escherichia coli* M15 and purified under nondenaturing conditions. Fractions were collected and analyzed with sodium dodecyl sulfate polyacrylamide gel electrophoresis (SDS-PAGE) and stored in the elution buffer at 4 °C in stable conditions for at least several months. The $(His)_6$ExpR protein was immobilized on the succinimide-activated mica surface by a short linker molecule coupled to one of the 11 ExpR lysine residues.

The DNA target sequence was a 313 bp DNA fragment and included 97 bp flanking sequences derived from the pUC18 vector, 31 bp of the 3′ end of *sinR*, the 156 bp of the *sinR*−*sinI* intergenic region, and 29 bp of the 5′ end of *sinI*, and was characterized with electrophoretic mobility shift assays (EMSA). The DNA fragment was attached to the tip via the PEG polymer spacer. Seven AHL autoinducers, C_7-HL, C_8-HL, C_{10}-HL, C_{12}-HL, oxo-C_{14}-HL, $C_{16:1}$-HL, and C_{18}-HL, were either purchased (Sigma-Aldrich) or synthesized.

(21) Zhou, S.; Hempenius, M. A.; Schönherr, H.; Vancso, G. J. *Macromol. Rapid. Commun.* **2006**, *27*, 103−108.
(22) Grandi, F.; Sandal, M.; Guarguaglini, G.; Capriotti, E.; Casadio, R.; Samorì, B. *ChemBioChem* **2006**, *7*, 1774−1782.
(23) Hutter, J. L.; Bechhoefer, J. *Rev. Sci. Instrum.* **1993**, *7*, 1868−1873.
(24) Evans, E.; Ritchie, K. *Biophys. J.* **1997**, *72*, 1541−1555.
(25) Merkel, R.; Nassoy, P.; Leung, A.; Ritchie, K.; Evans. E. *Nature* **1999**, *397*, 50−53.

(b) The synthesis, purification, and characterization of the supramolecular resorcin[4]arene host systems (2,8,14,20-tetra-(10-(decylthio)decyl) cavitand and its photoswitchable anthracene-modified derivative) have been described elsewhere.[18−19] Both resorcin[4]arenes can be surface-immobilized in an oriented manner via the four dodecyl sulfide linkers on gold by molecular self-assembly in ethanol solutions.

Results and Discussion

Regulated Protein−DNA Interaction. First, we investigated a naturally occurring, population density-dependent gene regulation process in *S. meliloti* that is controlled by low molecular-weight compounds called autoinducers or effectors, which is referred to as quorum sensing (QS). QS is known to regulate many different physiological processes, including the production of secondary metabolites, conjugal plasmid transfer, swimming, swarming, biofilm maturation, and virulence in human, plant, and animal pathogens.[26] Many QS systems involve AHLs as signal molecules that vary in length, degree of substitution, and saturation of the acyl chain. Since bacterial cell walls are permeable to AHLs, they can accumulate both intracellularly and extracellularly, and, once a threshold concentration is reached, they act as co-inducers, usually by activating LuxR-type transcriptional regulators upon recognition and binding.

In our AFM force spectroscopy experiments, the binding partners $(His)_6$ExpR and the respective 313 bp DNA fragment were covalently bound to the sample surface and to the AFM tip, respectively (Figure 1a). When approaching the tip to and retracting it from the surface, the flexibility of the polymer linker allowed the DNA molecules to access the binding domains of the immobilized $(His)_6$ExpR proteins. The binding or association can be verified during mechanical withdrawing of the AFM tip from the surface by a characteristic stretching of the polymer linker molecule, the build-up of an attractive interaction force, and a subsequent snapping back to zero force (Figure 1b). In these force−distance curves, the measured force acting on the AFM tip against the vertical position (given by the extension of the piezo actuator) are plotted. Since these dissociation processes are of stochastic nature and obey the laws of a thermally activated decay of a metastable state[24] the measured dissociation forces from multiple approach−retract cycles (at constant retract velocity) vary in a (well-defined) statistical manner and can be combined in a force histogram. In the case of a total absence of AHL effector molecules in the buffer solution, the total activity or binding probability (# events/# cycles) remained below 0.5%, and the force histogram consisted only of rare and unspecific scattered events (Figure 1c). The histogram profile changed drastically when AHL was added to the buffer solution (Figure 1d: 10 μM oxo-C_{14}-HL). The measured dissociation forces form a distribution of almost Gaussian shape with the most-probable dissociation force of about 60 pN and the total binding probability increased to 8−10%. These experiments suggest that ExpR binds to DNA only in very rare and unspecific cases in the absence of any effector, whereas the probability of association and binding is increased in the presence of an appropriate AHL effector by a factor of ∼20.

In order to verify the specificity of the interaction, competition, and control experiments with free specific DNA binding fragments (10 ng/μL) and unspecific Epstein−Barr virus nuclear antigen (EBNA)−DNA fragments, which lack the binding sequence, were performed. All these results were clearly indicative of specific binding between the $(His)_6$ExpR and its specific DNA binding sequence (data not shown).[15]

(26) Williams, P.; Winzer, K.; Chan, W. C.; Camara, M. *Philos. Trans. R. Soc. London, Ser. B* **2007**, *362*, 1119−1134.

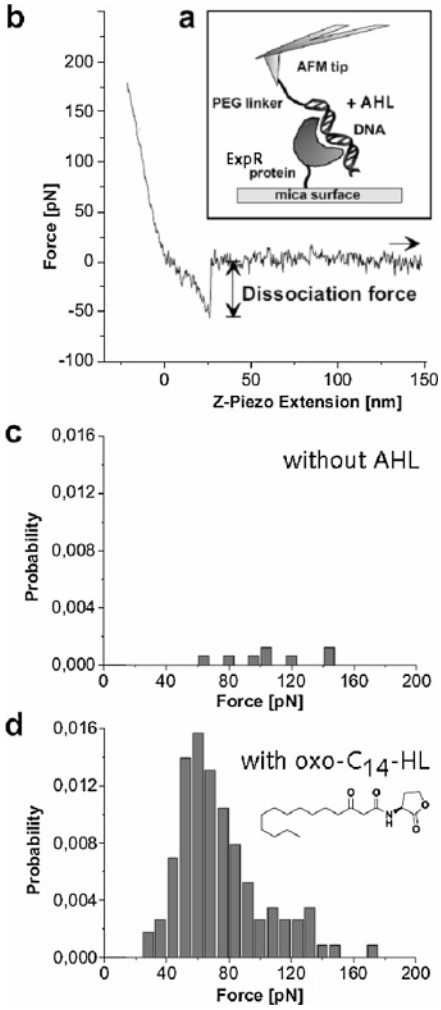

Figure 1. Force spectroscopy measurements on AHL-mediated DNA−$(His)_6$ExpR interaction. (a) DNA fragments are attached to Si_3N_4 AFM tip via PEG spacer molecules, and the $(His)_6$ExpR proteins are immobilized on a flat mica surface. (b) Typical force−distance curve with ExpR−DNA/+AHL binding event while the tip was retracted from the sample surface at constant velocity. (c) Force histogram of dissociation forces for the DNA−$(His)_6$ExpR complex without effector (at v = 2000 nm/s) corresponding to the inactive non-affine state and (d) after adding 10 μM of *N*-(3-oxotetradecanoyl)-L-homoserine lactone (oxo-C_{14}-HL), yielding full binding affinity. (Figure adapted from ref 15).

In order to investigate the binding heterogeneity on AHL-type molecules, seven different AHL effectors were studied in detail by AFM DFS. It turned out that, of seven effectors tested, six (C_8-HL, C_{10}-HL, C_{12}-HL, oxo-C_{14}-HL, $C_{16:1}$-HL, and C_{18}-HL) were able to stimulate protein−DNA binding. One, C_7-HL, the effector with the shortest chain length, yielded no noticeable activity when added to the buffer solution. In Figure 2 the DFS result of the C_{12}-HL-stimulated $(His)_6$ExpR−DNA binding is presented in a force diagram where the measured dissociation forces are plotted against the varied loading rates, and display the theoretical predicted linear dependence. In this respect, we quantitatively characterized all six active AHL effectors and plotted the calculated parameters reaction length x_β, the dissociation rate constant k_{off}, and the interaction lifetime τ in Figure 3. The parameters distinctively differ and show a non-monotonous dependence of bond lifetime on AHL chain length with C_8-HL as the complex with the longest lifetime. Obviously, the change of the AHL acyl chain length by one C atom (C_7-HL to C_8-HL) is sufficient to activate the binding between ExpR and its DNA binding sequence. In order to learn about the binding mechanism

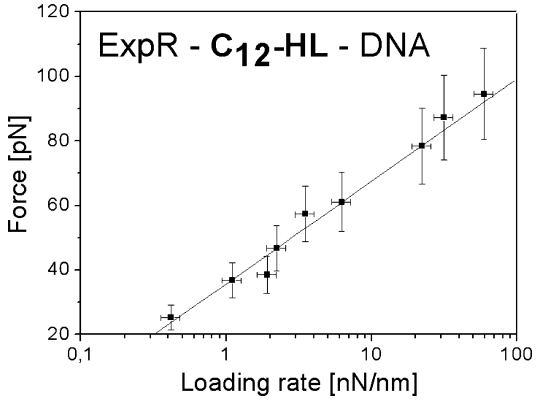

Figure 2. AFM DFS of the $(His)_6$ExpR−DNA interaction in the presence of the C_{12}-HL effector. Plot of the measured dissociation forces against the logarithm of the loading rate r upon systematical variation of the retract velocity, where $r =$ (effective spring constant of the molecular complex) × (retract velocity). Extrapolating the line fit to the state of zero external force yields the natural thermal off-rate constant k_{off}. (Figure adapted from ref 15).

HL	Reaction length x_β [Å]	Off-rate k_{off} [s^{-1}]	Mean lifetime [ms]
C_8	5.7 ± 0.3	0.48 ± 0.16	2273 ± 758
C_{10}	5.2 ± 0.3	1.43 ± 0.45	699 ± 220
C_{12}	2.9 ± 0.2	5.40 ± 1.03	185 ± 35
oxo-C_{14}	3.5 ± 0.3	3.48 ± 0.62	287 ± 51
$C_{16:1}$	3.9 ± 0.6	2.19 ± 1.88	457 ± 392
C_{18}	4.7 ± 0.8	1.32 ± 1.27	758 ± 729

Figure 3. Molecular interaction parameters k_{off}, mean lifetime τ, and x_β for $(His)_6$ExpR protein binding to its DNA target sequence under the various probed AHL effectors as derived from DFS. (Figure adapted from ref 15).

of this interaction and the reason for this abrupt change in affinity by AHL acyl chain length, the interaction was investigated by additional competition experiments (Figure 4). First, we probed the ExpR−DNA complex in the presence of C_7-HL, yielding a force histogram lacking significant specific activity, dominated by spurious nonspecific interaction (Figure 4a). After removing C_7-HL from the buffer solution by multiple washing steps with AHL-free buffer solution for 1 h, the addition of C_{12}-HL only resulted in minor activation of ExpR (Figure 4b), in contrast to the expected characteristics reported above. This was indicative of a long-living ExpR−C_7-HL complex that inhibited activation by C_{12}-HL. Second, and by reversing the experiment, a different response was found. The fresh (new tip and new sample!) ExpR−DNA complex was now probed in the presence of C_{12}-HL, yielding the expected strong and specific activity in the force histogram (Figure 4c). After removing C_{12}-HL now from the buffer solution, the addition of C_7-HL only marginally reduced this activity, and the complex still showed a considerable degree of activity in the presence of C_7-HL, which was indicative of a long-living and C_{12}-HL-activated complex (Figure 4d). Overall, it can therefore be concluded that the lifetime of the protein−effector bond is much larger than the lifetime of the effector-mediated ExpR−DNA binding. The ExpR−DNA binding kinetics can therefore be regarded as AHL−ExpR kinetic independent, indicating that only the structural change invoked by the binding of a particular AHL effector molecule is able to induce the relevant DNA−protein interaction and to regulate the associated expression process.

Since AFM DFS operates at the level of individual molecular complexes, it is independent of the variations in solubilities due

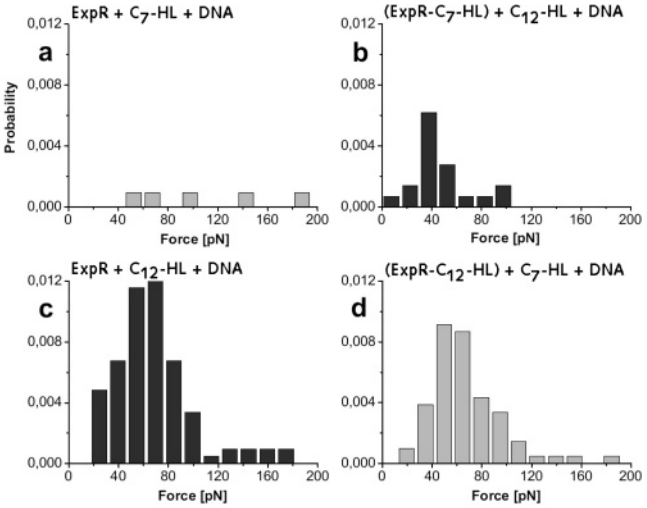

Figure 4. Stability of the protein−effector bond in competition experiments. (a) In the presence of C_7-HL, no specific binding is observed. (b) After the sample was washed with plain buffer solution and C_{12}-HL was added, the protein−DNA complex remained inactive. (c) The reversed process was investigated first in the presence of C_{12}-HL, where the protein−DNA complex shows its expected full degree of activity. (d) C_7-HL was added after the sample was washed with plain buffer, and the activity was only marginally reduced. Both experiments indicate the high stability and long lifetime of the protein−effector bond. (Figure adapted from ref 15).

to differences in the acyl chain length of the effectors, and allows the quantitative investigation of this regulation and molecular switching phenomenon, giving even access to details in the mechanism of the binding process.

Supramolecular Photochemical Single-Molecule Affinity Switch. In order to mimic this molecular switching function with an artificial organic system, we designed supramolecular organic constituents, which interact noncovalently in a directed and specific way to host−guest complexes of higher complexity. The ability to tailor the molecular interplay with respect to chemical design, specificity, and molecular switching opens fascinating concepts for the development of new molecular materials for artificial molecular recognition, molecular organization, and self-assembly. We chose resorcin[4]arene (calixarene) ligand host−guest complexes as model receptor systems, providing synthetic receptor cavities for the inclusion of small cationic guests such as alkali or ammonium ions and even neutral compounds.[27−28] Organic cations such as ammonium ions play significant roles in molecular recognition processes in nature (e.g., in protein side chains) and interact by ion−dipole interactions, hydrogen bonds, and cation−π interactions between the positive charge of the ion and the host molecules often containing arene units.

The specificity of the binding is governed by the topological complementarity of the host and guest: only cations small enough to fit into the tailored cavity are recognized by the resorcin[4]-arene. In our experiments, 2,8,14,20-tetra-(10-(decylthio)decyl) cavitands with a calculated cavity width of 0.7 nm serving as a host receptor in an unmodified and with an anthracene-modified photoswitchable version were investigated in AFM DFS experiments in ethanol against the specific recognition of ammonium ions and ammonium ion derivatives (Figure 5a). First, the nonfunctionalized version of the resorcin[4]arene, a cavitand

(27) Gutsche, C. D. *Calixarenes Revisited*; Royal Society of Chemistry: Cambridge, U.K., 1998.
(28) Mandolini, L.; Ungaro, R. *Calixarenes in Action*; Imperial College Press: London, 2000.

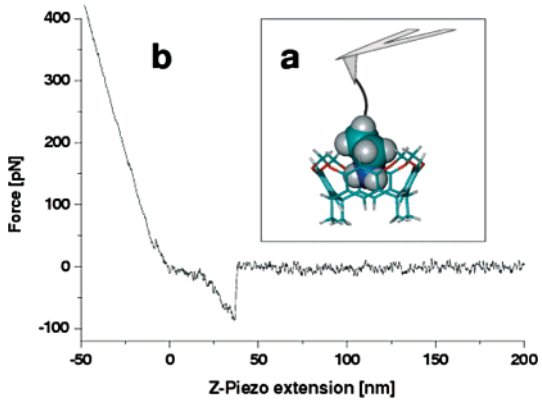

Figure 5. (a) Force spectroscopy scheme for measuring the interaction between the ammonium-activated Si_3N_4 AFM tip and the supramolecular resorcin[4]arene cavitand immobilized on a gold surface. The ammonium ion is attached to a Si_3N_4 AFM tip via a flexible polymer cross-linker and represented together with the complex between the cavitand and an ethyl ammonium cation taken from a quantum chemical gas-phase calculation. (b) Typical force−distance curve with molecular dissociation event of this supramolecular host−guest system (only retractive trace is shown). (Figure adapted from ref 18).

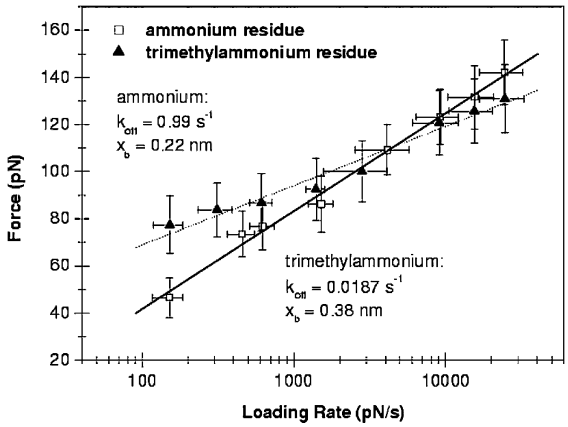

Figure 6. AFM DFS. Plot of the measured dissociation forces against the logarithm of the loading rate *r*. Upon systematical variation of the retract velocity, complexes formed by the resorcin[4]arene cavitand and different ammonium guests were quantitatively investigated. For details see text. (Figure adapted from ref 18).

was investigated. In Figure 5b, a typical force curve of a molecular dissociation event between the cavitand and an ammonium ion is plotted. The nonlinear elastic stretching of the PEG spacer before the point of dissociation served as the criterion to discriminate real single binding events from unspecific adhesion, and gives information about the overall elasticity of the molecular complex. This cavitand was probed against ammonium, trimethyl ammonium and triethyl ammonium cations in AFM DFS experiments.[18] The loading rate-dependent experiments were plotted in force histograms where the respective dissociation forces have been determined (data not shown).[16] Interestingly, the ammonium and trimethyl ammonium residues clearly exhibited a distinct and concise affinity toward the resorcin[4]-arene cavitand (total binding probability ≈ 25%), whereas the triethyl ammonium ion did not display any affinity, because of its molecular size (0.8 nm), which exceeds the width of the binding cavity. The unequivocal evidence for the specificity of the interaction was cross-checked with respective competition and blocking experiments.[18]

In Figure 6, the force loading rate plots reveal details about the kinetics of the unbinding and information concerning the

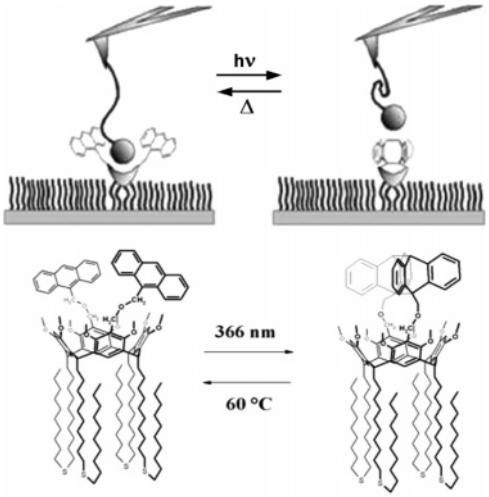

Figure 7. Pictograms visualizing the diluted self-assembled monolayer of this resorcin[4]arene photoswitch for AFM single-molecule affinity studies and the photochemical switching cycle. For details see text. (Figure adapted from ref 19).

reaction length, yielding $k_{off} = (0.99 \pm 0.81)\ s^{-1}$ for the ammonium and $k_{off} = (1.87 \pm 0.75) \times 10^{-2}\ s^{-1}$ for the trimethyl ammonium residue, resulting in complex lifetimes of $\tau = 1.01$ s and $\tau = 53.5$ s, respectively. The respective reaction lengths were determined to be $x_\beta = (0.22 \pm 0.04)$ nm for ammonium, and $x_\beta = (0.38 \pm 0.06)$ nm for the trimethyl ammonium ions. These figures qualitatively scale well with the calculated van der Waals diameters of 0.3 nm for ammonium and 0.6 nm for trimethyl ammonium, respectively.[29] This suggests a direct and considerable contribution of hydrogen bonds (not present in the trimethyl ammonium cavitand interaction) and cation−π interactions to the molecular binding mechanism. Especially for the trimethyl ammonium cavitand system, the latter contribution may be dominant because of its positive charge distribution, which is known to be located on the hydrogen atoms of the methyl groups.[30−31]

On the basis of this 2,8,14,20-tetra-(10-(decylthio)decyl) cavitand, we synthesized a bistable, photoswitchable resorcin-[4]arene that was modified with two anthracene units in opposite positions at the upper resorcin[4]arene rim and proved its switching functionality in ensemble photochemical induction and heating cycles.[32−33] This compound can repeatedly be switched by photodimerization of the two anthracenes between the open and closed isomers in ethanol by irradiation with UV light (360−370 nm), or vice-versa by UV irradiation below 270 nm or by the transfer of thermal energy (Figure 7). The affinity switching was investigated by AFM single-molecule force spectroscopy against an ammonium cation guest molecule. Five series of force spectroscopy experiments were recorded (Figure 8a−d). The first series was measured on the open and active isomer, i.e., after heating. The corresponding force histogram is given in Figure 8a, yielding an overall binding probability of 9.1% with a dissociation force of 101 pN at a loading rate of 5260 pN s^{-1}. Then the sample was irradiated with UV light, and, subsequently, a new force spectroscopy series was recorded.

(29) Rozhenko, A. B.; Schoeller, W. W.; Letzel, M. C.; Decker, B.; Agena, C.; Mattay, J. *Chem.—Eur. J.* **2006**, *12*, 8995−9000.
(30) Deakyne, C. A.; Meot-Ner (Mautner), M. *J. Am. Chem. Soc.* **1985**, *107*, 474−479.
(31) Schneider, H. J.; Schiestel, T.; Zimmermann, P. *J. Am. Chem. Soc.* **1992**, *114*, 7698−7703.
(32) Azow, V. A.; Schlegel, A.; Diederich, F. *Angew. Chem., Int. Ed.* **2005**, *44*, 4635−4638.
(33) Schäfer, Ch.; Mattay, J. *Photochem. Photobiol. Sci.* **2004**, *3*, 331−333.

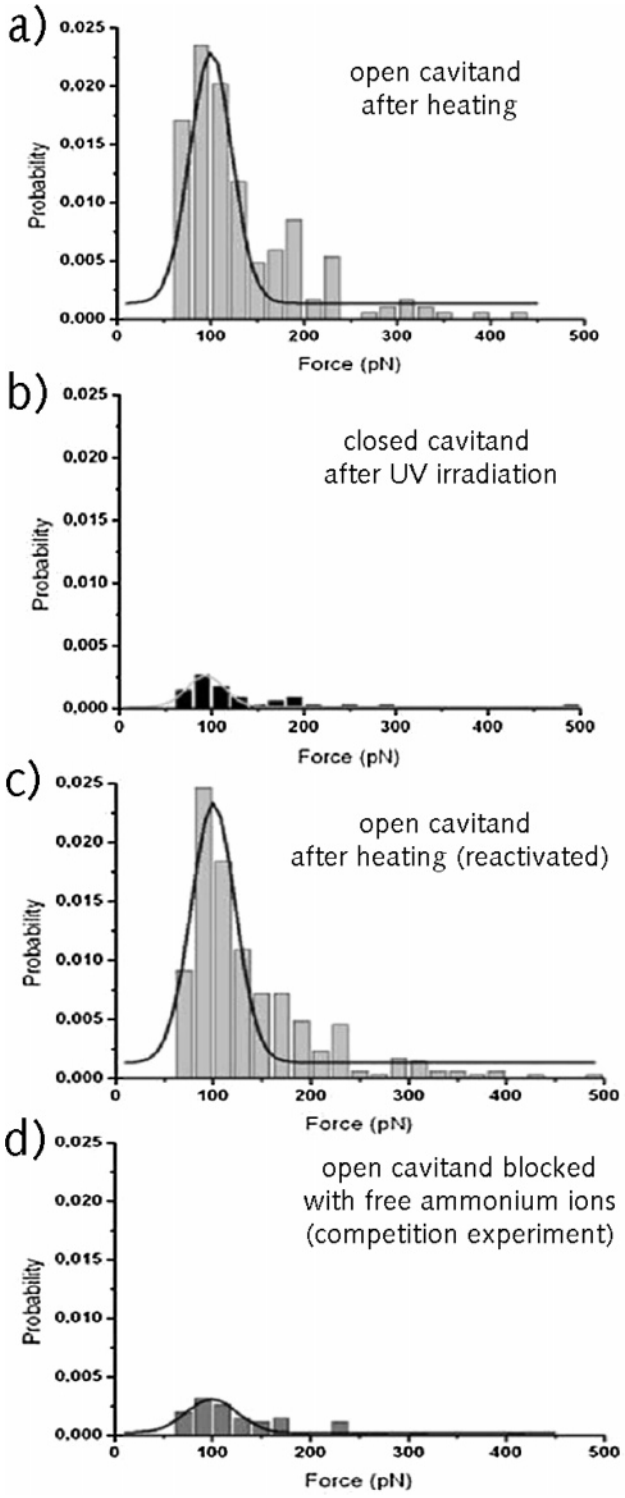

Figure 8. AFM single-molecule force spectroscopy experiments with the resorcin[4]arene photoswitch. (a) Force histogram of experimental series after heating the sample to 60 °C for 2 h, yielding an active (open) resorcin[4]arene with full activity against ammonium ions and a mean dissociation force of 101 pN. (b) Force histogram of series after irradiating the sample at 368 nm for 5 min, yielding an inactive (closed) resorcin[4]arene. (c) Force histogram after renewed heating of the sample for 2 h, yielding a reactivated (open) resorcin[4]arene with full activity against ammonium ions and a mean dissociation force of 99 pN. (d) Force histogram of a competition experiment, performed in ethanol solution where the sample surface was fully saturated with free ammonium, yielding an inactive (closed) cavitand. All experiments were performed with the same AFM tip and sample taken at a retract velocity of 1000 nm s^{-1}. (Figure adapted from ref 19).

The corresponding force histogram is shown in Figure 8b. The binding probability was significantly lowered after irradiation to 0.9%, reflecting the closing of the cavitands by the UV exposure. The very small number of remanent events might be either associated to incomplete closing or gradual reopening of the system. For the next series (Figure 8c), the sample was heated again for 2 h. The resulting force histogram closely resembles the first one (Figure 8a), yielding a total binding probability of 9.6%, indicating that the reopening of the supramolecular host system was successful. In the following experimental series, a competition experiment in ethanol saturated with ammonium chloride was conducted (Figure 8d). The competition significantly lowered the overall binding probability (to 1.4%), although not to the extent that was observed after UV radiation. After washing the sample with ethanol, a last experimental series was performed, which again closely resembled the first one (data not shown). The overall binding probability for the open system without competitor could be fully recovered (9.5%), indicating a complete and reversible reactivation of the molecular affinity.

These AFM DFS experiments prove that the resorcin[4]arene derivate can be reversibly switched between two different bistable isomeric configurations, which can be probed reproducibly and reversibly at the single-molecule level, which mimics the functional affinity and binding properties of the effector-mediated transcriptional activator ExpR.

Conclusion

The characterization of the molecular switching properties in a naturally occurring molecular system such as effector-mediated ExpR−DNA interaction and its reverse engineered supramolecular resorcin[4]arene cavitand at the single-molecule level with AFM force spectroscopy proved the ability of this quantitative interaction force technique to be used as a sensitive tool for a sophisticated binding analysis of complex (multiple-component) systems. AFM DFS quantitatively accesses molecular interaction forces, elasticities, binding landscapes, kinetic rate constants, and, last but not least, an estimate of binding energies. This allows a quantitative affinity ranking of intermolecular interaction with a sensitivity of single point mutations or atomic variations under liquid and physiological environment in an affinity range of $K_d = 10^{-5}$ M (supramolecular host−guest systems)[18] to 10^{-15} M (streptavidin−biotin).[4] In addition, the relevant physical mechanisms of the binding and switching process can be investigated, which gives novel and deep insight into the structure−function relationship of the molecules involved.

In the future, other bistable and externally controlled (bio)-molecular receptor−ligand systems for molecular manipulators, nanoscale rewritable molecular memories, and regulated artificial ion channels, which will serve for a controlled transport and release of ions and neutral compounds will be functionally investigated with AFM DFS.

Acknowledgment. The authors acknowledge manifold support and contributions from Ceno Agena, Alexander Fuhrmann, Matthias C. Letzel, Christoph Metzendorf, Christoph Pelargus, Alfred Pühler, Alexander B. Rozhenko, Wolfgang W. Schoeller, Katja Tönsing, and Volker Walhorn. Financial support from the Deutsche Forschungsgemeinschaft within the Collaborative Research Center "Physics of Single Molecule Processes and Molecular Recognition in Organic Systems" (SFB 613) is gratefully acknowledged.

LA702373B